



Published in final edited form as:

Mol Cell Endocrinol. 2011 June 6; 339(1-2): 151–158. doi:10.1016/j.mce.2011.04.007.

Hypothalamic but not pituitary or ovarian defects underlie the reproductive abnormalities in *Axl/Tyro3* null mice

Angela Pierce^{1,3}, Mei Xu^{1,3}, Brian Bliesner^{1,3}, Zhilin Liu⁴, JoAnne Richards⁴, Stuart Tobet⁵, and Margaret E. Wierman^{1,2,3}

¹Department of Medicine, University of Colorado Denver School of Medicine, Aurora, CO 80045

²Department of Physiology and Biophysics, University of Colorado Denver School of Medicine, Aurora, CO 80045

³Research Service VAMC, Denver, CO 80220

⁴Department of Cell Biology, Baylor College of Medicine, Houston TX 77030

⁵Department of Biomedical Sciences, Colorado State University, Fort Collins, CO 80523

Abstract

AXL and TYRO3, members of the TYRO3, AXL and MER (TAM) family of tyrosine kinase receptors, modulate GnRH neuronal cell migration, survival and gene expression. *Axl/Tyro3* null mice exhibit a selective loss of GnRH neurons, delayed sexual maturation and irregular estrous cycles. Here we determined whether the defects were due to direct ovarian defects, altered pituitary sensitivity to GnRH and/or an impaired LH surge mechanism. Ovarian histology and markers of folliculogenesis and atresia as well as corpora luteal development and ovarian response to superovulation were not impaired. *Axl/Tyro3* null mice exhibited a robust LH response to exogenous GnRH, suggesting no altered pituitary sensitivity. Ovariectomized *Axl/Tyro3* null mice, however, demonstrated an impaired ability to mount a steroid-induced LH surge. Loss of GnRH neurons in *Axl/Tyro3* null mice impairs the sex hormone-induced gonadotropin surge resulting in estrous cycle abnormalities confirming that TAM family members contribute to normal female reproductive function.

Keywords

GnRH; Axl; Tyro3; LH surge; ovary

Introduction

Members of the TAM family of receptor tyrosine kinases (TYRO3, AXL and MER) contain an intracellular kinase and an extracellular ligand binding domain with characteristics of a neural cell adhesion molecule including fibronectin and immunoglobulin repeats (Lai and Lemke, 1991, Lemke and Rothlin, 2008, Linger, 2007). Growth arrest specific gene 6

Corresponding author: Margaret E Wierman, University of Colorado at Denver, Endocrinology MS8106, 12801 East 17th Ave, RC1 South, Aurora, CO 80045 Phone: 303-724-3952, Fax: 303-393-5271, margaret.wierman@ucdenver.edu.

Publisher's Disclaimer: This is a PDF file of an unedited manuscript that has been accepted for publication. As a service to our customers we are providing this early version of the manuscript. The manuscript will undergo copyediting, typesetting, and review of the resulting proof before it is published in its final citable form. Please note that during the production process errors may be discovered which could affect the content, and all legal disclaimers that apply to the journal pertain.

Disclosure Summary: The authors have nothing to disclose

(GAS6), and in some tissues the closely-related Protein S (ProS1), are ligands for the TAM family members (Manfioletti, Brancolini, Avanzi et al., 1993, Hafizi and Dahlback, 2006). Analysis of TAM expression in immortalized GnRH neuronal cells showed that *Axl* and *Tyro3* (but not *Mer*) mRNA and protein are expressed in NLT cells, a model of migrating GnRH neurons, while *Tyro3* and *Mer* are expressed in post-migratory GT1-7 GnRH neuronal cells (Fang, Xiong, James et al., 1998). We hypothesized that AXL and TYRO3 may mediate GnRH neuron migration and/or survival and impact on the ontogeny of the GnRH neuronal network during development (Allen, Linseman, Udo et al., 2002, Allen, Zeng, Schneider et al., 1999).

Previously, we determined the reproductive consequences of disrupting both the *Axl* and *Tyro3* genes in female mice (Pierce, Bliesner, Xu et al., 2008). Overall fertility, birth rates, and age at vaginal opening of the mutant mice were similar to WT, but *Axl/Tyro3* null mice showed delayed first estrous and consistently impaired estrous cycles. Cycles were irregular and prolonged with an increased percentage of days in proestrous. Immunoblots of homogenates from brain regions dissected from WT embryos at embryonic day 15 (E15) revealed that AXL and TYRO3 were expressed in the developing hypothalamus. In contrast, TYRO3 and MER, but not AXL were expressed in adult WT hypothalamus, consistent with a role for AXL and TYRO3 in the early development of GnRH neurons. Compared with WT, *Axl/Tyro3* null adults exhibited a 34% loss in the number of immunoreactive GnRH neurons in the region of the organum vasculosum of the lateral terminalis (OVLT), previously shown to be important for the GnRH-induced LH surge in rodent species (Adachi, Yamada, Takatsu et al., 2007, Herbison, 2008, Mayer, Acosta-Martinez, Dubois et al., 2010). Together these data supported a central defect in GnRH neuronal development contributing to the reproductive phenotype.

In the current study we sought to determine whether the reproductive abnormalities were due to concomitant peripheral as well as central defects. Because other studies suggested TAM family members were expressed in rodent and human gonads (Lu, Gore, Zhang et al., 1999, Schulz, Paulhiac, Lee et al., 1995, Wang, Chen, Ge et al., 2005, Wu, Tang, Chen et al., 2008), we examined markers of folliculogenesis and luteal function, ovarian TAM expression and the response to a standard superovulation protocol. We assessed pituitary function and also determined if the localized loss of GnRH neurons in *Axl/Tyro3* null mice impaired the LH surge mechanism in response to sex steroids.

Materials and Methods

Mice

Axl and *Tyro3* null mice established in a C57BL/6 × 129sv background (Lu et al., 1999) were bred to create *Axl/Tyro3* null mice. Control C57BL/6 × 129sv mice were purchased from The Jackson Laboratory (Bar Harbor, Maine). Animal care and experimental procedures were performed in accordance with the guidelines established by the Denver Veterans Affairs IACUC. Female and male mice were housed in micro-isolator cages in the same room under a 12 hour light cycle with food and water *ad libitum*. All mice were genotyped by PCR analysis of tail DNA as previously described (Pierce et al., 2008). Mice were anesthetized with isoflurane from Webster Veterinary Supply (Sterling, MA) and sacrificed by cervical dislocation for tissue and blood collection. For major surgeries, anesthesia was induced with a cocktail of ketamine (80 mg/kg body weight) (Hospira, Inc, Lake Forest, IL,) and xylazine (10 mg/kg body weight) (Lloyd Labs, Shenandoah, IO) injected intraperitoneally and maintained with isoflurane as needed.

Reagents

Axl (M-20) antibody and horseradish peroxidase (HRP)-linked anti-goat antibody were purchased from Santa Cruz Biotechnology (Santa Cruz, CA). Tyro3 antiserum was a generous gift from Cary Lai at The Scripps Research Institute. Mer antibody was purchased from R&D Systems (Minneapolis, MN). Gas6 antibody was obtained from Bryan Varnum at Amgen (Thousand Oaks, CA). GAPDH antibody was purchased from Millipore (Billerica, MA). HRP-conjugated secondary antibodies (Donkey anti-rabbit IgG and sheep anti-mouse IgG) were purchased from GE Healthcare Bio-Sciences Corp (Piscataway, NJ).

RT-PCR

Ovaries and pituitaries from adult mice were collected in RNAlater from Ambion (Austin, TX). RNA was purified using TRIzol Reagent from Invitrogen (Carlsbad, CA) or Qiagen RNeasy mini kit (Valencia, CA). RNA (1.0 µg) was reverse transcribed using Thermo Verso cDNA kit from Fisher (Pittsburgh, PA). RT-PCR was performed under the following conditions: 94°C for 3 min; 94°C for 45 sec, 54°C for 45 sec, and 72°C for 1 min for 35 cycles; 72°C for 10 min. Primer sequences for amplifying *Axl* were: 5'-CCCCTGAGAACGTTAGCG-3' and 3'-TGCTCTGCAGTACCATCTAGC-5'. The primer sequences for amplifying *Tyro3* were: 5'-CGATCTCCAGCTACAACGC-3' and 3'-GCATGGCTGAGTCCGGAAT-5'. The primer sequences for amplifying *Mer* were: 5'-CTGCACAGTGAGAATCGCG-3' and 3'-GCCTGGCTCAGATGTGTTCG-5'. Primer sequences for amplifying *Gas6* were: 5'-CCAGACCTGCCAAGATATCG-3' and 3'-GCCATGTTACCGCAACCC-5'. The quantity of *Axl*, *Tyro3*, *Mer*, and *Gas6* mRNA was normalized to that of glyceraldehyde-3-phosphate dehydrogenase (*GAPDH*) mRNA. The primer sequences for amplifying *GAPDH* were: 5'-CGACCCCTTCATTGACCTCA-3' and 3'-GCCACGACTCATAACAGCACC-5'. The primer sequences for amplifying ovarian RNA are: *Foxo1-F*: 5'-GTGAACACCATGCCTCACAC-3', *Foxo1-R*: 5'-TGGACTGCTCCTCAGTTCCT-3'; *Sfrp4-F*: 5'ATGCTCCGCTCCATCCTGGTG-3', *Sfrp4-R*: 5'-TGGCCAGGATGGCGTTTCTCC-3'; *Cyp11a1-F*: 5'-GTACTTGGGCTTTGGCTGGG-3' *Cyp11a1-R*: 5'-CAGGTCCTGCTTGAGAGGCT-3'. Ovarian RNA was normalized to the ribosomal protein L19 using specific primer pairs: *Rpl19-F* 5'GGTGACCTGGATGAGAAGGA and *Rpl19-R* 5'-TTCAGCTTGTGGATGTGCTC.

Immunoblots

Tissues were homogenized in 1× RIPA buffer (150 mM NaCl, 1% NP-40, 0.5% deoxycholate, 0.1% SDS, 59 mM Tris, pH 8.0) from Upstate (Lake Placid, NY) with freshly added 0.5 mM PMSF (Sigma-Aldrich, St. Louis, MO), 1× protease inhibitor (Sigma-Aldrich, St. Louis, MO), 20 mM Na₃VO₄ and 25 mM NaF (Fisher, Pittsburgh, PA). Protein lysates were quantified using BCA assay (Pierce, Rockford, IL). An aliquot of 50 µg of total protein was resolved by 7.5% SDS/PAGE using a Bio-Rad mini-gel system (Bio-Rad, Hercules, CA). Proteins were transferred to Hybond polyvinylidene difluoride (Amersham, Arlington Heights, IL) using a Bio-Rad mini transblotter system. The membranes were blocked in 3% BSA in TBS-T buffer (20 mM tris-Cl, pH 7.6, 137 mM NaCl, 0.1% Tween-20) for 1 h at room temperature. Primary antibodies were diluted to 1:500 to 1:2000 in 0.5% BSA/0.1% NaN₃ in TBS-T and incubated with the membranes at 4°C overnight. The membranes were washed in TBS-T. The HRP-linked secondary antibodies were diluted to 1:3000 in TBS-T and incubated with the membranes for 1 h at room temperature. The membranes were washed and visualized using Enhanced Chemiluminescence (ECL) immunodetection reagents from Thermo Fisher Scientific, Inc (Rockford, IL).

Ovarian Histology and Analysis of Corpora Lutea

Ovaries from adult mice were collected in 10% formalin, sectioned and stained with hematoxylin and eosin (H&E). For estimation of average number of corpora lutea per cross-section, 3 to 7 mid-ovary sections from one ovary per mouse from 5 WT and 5 *Axl/Tyro3* null random cycling females were counted. For *in situ* hybridization analyses, ovaries of adult wild type ($n = 2$) and *Axl/Tyro3* null mice ($n = 3$) were fixed in 4% paraformaldehyde and embedded in paraffin. Sections (7 μm) were cut and processed for *in situ* hybridization using specific probes for genes expressed in luteal cells (*Cyp11a1*, *Sfrp4*) and granulosa cells and oocytes (*Foxo1*) as described previously (Robker and Richards, 1998, Richards, Sharma, Falender et al., 2002, Hsieh, Mulders, Friis et al., 2003). cDNA fragments of the relevant genes were amplified by RT-PCR from mouse ovarian total cDNA and sub-cloned into the pCR-TOPO4 vector (Invitrogen, Carlsbad, CA) (1–3). *In situ* hybridization was performed as previously reported. Tissue histology and the radioactive probes were visualized under light- and dark-field illumination, respectively, using a Zeiss AxioPlan2 microscope equipped with a 2.5 \times objective.

TUNEL Protocol

Paraffin-embedded ovary sections were deparaffinized and fixed in formaldehyde. Apoptotic follicles were identified using the DeadEnd™ Fluorometric TUNEL System (Promega Corp, Madison, WI). The percentage of growing follicles that stained positive for TUNEL was determined using a Nikon Eclipse E600 fluorescent microscope; images were acquired using Image ProPlus software

Superovulation Protocol

Female mice 28 to 34 days old were intraperitoneally injected with 5 IU Pregnant Mares Serum Gonadotropin (PMSG, Sigma-Aldrich, St. Louis, MO) on Day 1 and 5 IU or 2.5 IU human chorionic gonadotropin (hCG, Sigma-Aldrich) on Day 3. On Day 4, mice were anesthetized with isoflurane and sacrificed; both oviducts were dissected out onto a glass slide and ova were flushed from the ampulla with PBS and coverslipped. Ova were counted on a Nikon Diaphot microscope (Nikon Inc, Melville, NY) using a 10 \times or 20 \times objective.

Hormone Assays

Blood was obtained by terminal cardiac puncture from animals deeply anesthetized with isoflurane. Samples were allowed to clot at room temperature; serum was stored at -20°C until analysis. LH, FSH, estradiol and testosterone levels were assessed by radioimmunoassay performed by the Animal Reproduction and Biotechnology Laboratory at Colorado State University. Assay variations were as follows: estradiol intra-assay CV = 10.59%; inter-assay CV = 21.19%. LH intra-assay CV = 4.74%; inter-assay CV = 16.91%. Testosterone intra-assay CV = 6.62%; inter-assay CV = 14.19%. FSH intra-assay CV = 3.94%.

Pituitary (GnRH) Stimulation Protocol

Female mice between 2 and 3 months of age were injected subcutaneously with 200 ng/kg GnRH peptide (Sigma-Aldrich) in 100 μl saline. Blood was collected 10 minutes later by terminal cardiac puncture under anesthesia with isoflurane. Serum LH levels were measured and compared with LH in serum obtained from untreated controls; all blood was collected between 0800 and 1000 hr.

LH Surge Protocol

Mice between 2 and 3 months of age were bilaterally ovariectomized and implanted with Silastic® RX-50 Medical Grade Tubing (Dow Corning Corp, Midland, MI) filled with 17- β

estradiol (Sigma-Aldrich) dissolved in ethanol and mixed with Silastic® Medical adhesive Silicon, Type A (Dow Corning) at 0.1 mg/ml for final estrogen dosage of 1 µg/cm/20 g body weight. Mice were subcutaneously injected on Day 6 after implant with 1 µg estradiol benzoate (Sigma-Aldrich) dissolved in 100 µl of sesame oil (Sigma-Aldrich) and on Day 7 with 500 µg progesterone (Sigma-Aldrich) dissolved in 100 µl of sesame oil (Sigma-Aldrich). Mice were anesthetized with isoflurane (Webster Veterinary Supply) and blood collected by terminal cardiac puncture on Day 7.

Statistical Analyses

All data are expressed as a mean ± SEM for each group. Statistical differences between the means of two groups were tested using unpaired t-test. P-values were reported as “* <0.05 ”, “** <0.01 ” or “NS” (not significant). Statistical analyses were performed using GraphPad Software QuickCalcs Online Calculators for Scientists (www.graphpad.com, GraphPad Software, Inc, La Jolla, CA), Microsoft Office Excel 2003 v. 11 (Microsoft Corp, Redmond, WA) and SPSS Software (SPSS Inc, Chicago, IL).

Results

Axl, Tyro3 and Mer are expressed in WT mouse ovaries, but only Mer is expressed in Axl/Tyro3 null ovaries

Since TAM receptor protein expression has been reported in the gonads (Lu et al., 1999, Wang et al., 2005), we considered the possibility that a primary ovarian defect generated the reproductive phenotype and therefore analyzed TAM expression in WT and *Axl/Tyro3* null ovaries. Reverse transcriptase PCR (RT-PCR) was used to detect mRNA encoding TAM family members and their ligand, GAS6, in adult mouse ovary. Ovaries obtained from adult WT mice expressed abundant *Axl* and *Tyro3* transcripts, while *Axl/Tyro3* null ovaries expressed none (Fig. 1A), raising the possibility that an ovarian defect might contribute to the estrous irregularities in *Axl/Tyro3* null mice. Both ovaries expressed *Mer* and *Gas6* mRNAs. *Mer* mRNA expression was not up-regulated with the deletion of *Axl* and *Tyro3* in tissues. Immunoblots revealed AXL, TYRO3, MER and GAS6 protein were detected in WT ovaries; *Axl/Tyro3* null ovaries expressed MER and GAS6 as expected (Fig. 1B). Similar to mRNA levels, no changes in GAS6 or MER protein levels were observed in the *Axl/Tyro3* null samples compared with WT controls.

Ovarian morphology and expression of follicular and luteal cell markers in WT and Axl/Tyro3 null mice

Since TAM family members are expressed in granulosa cells (16), to address the possibility that loss of AXL and TYRO3 expression might contribute to ovarian dysfunction, we compared ovarian morphology and function in WT and experimental mice. Ovaries from randomly cycling WT and *Axl/Tyro3* null mice were examined and no differences in size, weight or appearance were observed. Corpora lutea were noted in ovaries from both genotypes. Microscopic examination of histological sections stained with hematoxylin and eosin revealed variable numbers of primordial, primary and antral staged follicles in both genotypes. No abnormal structures such as cysts were observed, and no indications of impaired follicle development were detected. Healthy and atretic follicles were identified in both genotypes.

To analyze follicular development in more detail, *in situ* hybridization was done to localize *Foxo1*, a transcription factor selectively expressed in oocytes and granulosa cells of growing follicles (Richards et al., 2002, Liu, Rudd, Hernandez-Gonzalez et al., 2009). *Foxo1* mRNA was highly expressed in granulosa cells and oocytes of WT and *Axl/Tyro3* null ovaries (Fig 2A). These ovaries contained more *Foxo1*-positive primary follicles as revealed by the

presence of *Foxo1* mRNA in oocytes (arrows in Fig. 2A). Antral follicles per section were not significantly different ($p=NS$) and real time RT-PCR analyses indicated that there were no differences in the expression of *Foxo1* mRNAs in *Axl/Tyro3* null ovaries compared to WT (Fig. 2B). Thus, there does not appear to be any major impairment of normal follicle development with deletion of *Axl* and *Tyro3*.

Since TAM family members have been shown to modulate rates of apoptosis in other tissues (Lemke and Rothlin, 2008, Pierce et al., 2008, Melaragno, Cavet, Yan et al., 2004), the numbers of atretic follicles were assessed by TUNEL in WT ($n = 4$) and *Axl/Tyro3* null ($n = 4$) ovaries (Fig. 2 C, D). The percentage of TUNEL-positive follicles varied from mouse to mouse (26 to 38% in WT, 29 to 41% in *Axl/Tyro3* null mice) but did not differ overall between groups ($34.3 \pm 2.78\%$ vs. $36.3 \pm 2.63\%$, respectively) (Fig. 2D). This is consistent with our finding that all stages of follicle development are present in *Axl/Tyro3* null ovaries.

To determine if the formation and/or function of corpora lutea were impaired, the numbers of corpora lutea and functional markers of luteal cells, *Cyp11a1* and *Sfrp4*, in WT and *Axl/Tyro3* null ovaries were compared. Mid-ovary sections from a single ovary were scanned and the number of corpora lutea per section was determined. Slightly fewer corpora lutea were observed in sections from experimental groups when compared with WT: 2.2 corpora lutea per section versus 2.7, respectively ($n=5$, $p=NS$) (Fig. 3A). Corpora lutea present in both groups expressed mRNAs encoding *Cyp11a1* and *Sfrp4* (Hsieh et al., 2003). Real time RT-PCR analyses indicated no significant differences in the expression levels of *Cyp11a1* or *Sfrp4* (Fig. 3B), although the intensity of the signals in the *Axl/Tyro3* null corpora lutea were variable (Fig. 3C). These results indicate that there are no major functional defects in corpora luteal function in *Axl/Tyro3* null mice.

Both WT and *Axl/Tyro3* null mice ovaries respond to an exogenous gonadotropin challenge

To confirm the lack of a functional ovarian defect, WT and *Axl/Tyro3* null mice were subjected to a standard superovulation protocol as described by Ojeda and coworkers (Prevot, Lomniczi, Corfas et al., 2005, Heger, Mastronardi, Dissen et al., 2007). Vaginal opening occurred at an average age of 34 d in both groups; first estrous occurred at day 35.4 in WT and day 39.7 d in *Axl/Tyro3* null mice (Pierce et al., 2008). Prepubertal female mice between 25 and 34 d old and matched for body weight were injected intraperitoneally with 5 IU PMSG and either 2.5 IU or 5.0 IU hCG to trigger ovulation. The number of ova recovered per mouse was counted under a dissecting microscope. The 7 WT and 8 *Axl/Tyro3* null mice that received the standard dose of 5 IU of hCG produced an average of 11.7 ± 1.6 and 9.1 ± 1.3 ova per mouse, respectively ($p = NS$). After administration of 2.5 IU hCG, 9.0 ± 1.2 and 6.3 ± 1.8 ova were released per mouse in 8 WT and 10 *Axl/Tyro3* null mice, respectively ($p = NS$) (Fig. 4). Thus, ovarian response to standard and sub-threshold doses of exogenous gonadotropins did not differ significantly between groups. More of the *Axl/Tyro3* null than WT mice released reduced numbers of ova (<5 per mouse) when injected with the low dose (2.5 IU) of hCG (5 of 10 or 50%, compared with 1 of 8 or 12.5% in WT) suggesting there may be subtle ovarian defects beyond the multiple measures assessed in our studies. By all indications, however, follicle development and ovulation were not severely impaired in *Axl/Tyro3* null ovaries.

Axl/Tyro3 null pituitaries respond to exogenous GnRH

To explore a potential pituitary defect in *Axl/Tyro3* null mice, studies examined TAM expression profiles in the pituitary and pituitary response to exogenous GnRH administration. Pituitary extracts collected from WT mice expressed ample levels of *Axl*, *Mer* and *Gas6* but low levels of *Tyro3* mRNAs. *Mer* and *Gas6* mRNAs were detected in

Axl/Tyro3 null mice, but not *Axl* and *Tyro3* (Fig. 5A). AXL protein was detected in WT pituitaries only; TYRO3 and MER proteins were undetectable in both groups. GAS6 protein was also expressed similarly in both genotypes (Fig. 5A). A GnRH stimulation test was then performed to assess the ability of pituitaries from *Axl/Tyro3* null mice to respond appropriately to exogenous GnRH. Serum was collected by terminal cardiac puncture from random cycling adult female mice at baseline or 10 minutes after the injection of 200 ng/kg of GnRH. Basal LH levels did not differ significantly between WT (0.38 ± 0.05 ng/ml; $n = 8$) and *Axl/Tyro3* null (0.47 ± 0.06 ng/ml; $n = 9$, $p = \text{NS}$; Fig. 5B). After GnRH stimulation, the LH levels rose significantly above baseline in mice of both genotypes and reached greater levels in *Axl/Tyro3* null mice than in WT mice [WT LH = 2.28 ± 0.27 ng/ml ($n = 8$), *Axl/Tyro3* null LH = 3.61 ± 0.48 ($n = 9$), $p < 0.05$]. These data show no evidence of a pituitary defect in *Axl/Tyro3* null mice and suggest a normal, albeit potentially heightened, response to GnRH at the level of the pituitary.

Hormone profiles in *Axl/Tyro3* null mice

To determine if basal reproductive hormone levels are altered, serum was obtained via cardiac puncture from adult female mice and LH and FSH levels measured (Fig. 5C). Basal LH levels were collected in the early morning from randomly cycling mice or mice in diestrous or proestrous. Although variable, there was no significant differences between random LH levels in WT (0.44 ± 0.04 ng/ml ($n = 12$)) and *Axl/Tyro3* null mice (0.48 ± 0.06 ng/ml, $n = 18$; $p = \text{NS}$). LH levels assayed on blood obtained from a subset of mice in diestrous did not differ between WT (0.32 ± 0.07 ng/ml, $n = 4$) and *Axl/Tyro3* null (0.50 ± 0.17 ng/ml, $n = 4$; data not shown). FSH levels were collected from randomly cycling females between 0800 and 1200 hr. FSH levels did not differ significantly between groups (*Axl/Tyro3* null -2.10 ± 0.67 ng/ml ($n = 5$)) compared to WT 2.54 ± 0.46 ng/ml ($n = 6$; $p = \text{NS}$). Estradiol levels were measured on samples from female mice (2.5 to 5 months of age) in diestrous or proestrous and did not differ significantly between WT (3.24 ± 1.43 pg/ml, $n = 8$) and experimental mice (2.30 ± 1.2 pg/ml $n = 8$, $p = \text{NS}$). LH, FSH, and estradiol levels were all within the reference normal ranges, demonstrating no dramatic alterations in basal gonadotropin or sex steroid levels with deletion of *Axl* and *Tyro3*. The lack of elevated FSH and/or LH levels in random cycling adult females is also supportive of the lack of a significant primary ovarian defect.

Effects of ovariectomy on LH levels in WT and *Axl/Tyro3* null mice

To assess the ability to mount a post-ovariectomy (post-OVX) rise in gonadotropins, LH levels were measured at baseline or 1 or 7 days after ovariectomy in *Axl/Tyro3* null and WT mice. LH levels increased significantly in both groups 7 days after ovariectomy ($p < 0.01$) (Fig. 5D). At Day 7 post-OVX, LH levels were 2.60 ± 0.31 ng/ml in WT mice ($n = 4$) compared with 2.74 ± 0.81 ng/ml in *Axl/Tyro3* null mice ($n = 6$, $p = \text{NS}$). These results suggest that endogenous estrogens are effective at negatively regulating LH levels in *Axl/Tyro3* null mice and indicate that the removal of the primary estrogen source permits a gonadotropin rise comparable to that observed in WT mice.

Axl/Tyro3 null mice have impaired positive feedback and LH surge mechanism

To test the hypothesis that the site-specific loss of GnRH neurons shown in *Axl/Tyro3* null mice would impair the sex steroid-induced LH surge, mice 2 to 3 months of age were ovariectomized and implanted with silastic implants containing $1 \mu\text{g/cm}^2/20\text{g}$ body weight $17\text{-}\beta$ estradiol for 7 days (Fig. 6). Subcutaneous injections of estradiol benzoate ($1 \mu\text{g}$ in $100 \mu\text{l}$ sesame oil) on Day 6 and progesterone ($50\mu\text{g}$ in $100 \mu\text{l}$ sesame oil) on Day 7 were administered to simulate the rise in sex steroids that trigger an LH surge in normal mice using a protocol optimized by Herbison and coworkers (Herbison, Porteous, Pape et al., 2008). Blood was obtained via terminal cardiac puncture on Day 7 in separate groups of

animals sacrificed hourly across the afternoon from 1500–1800 h to assess the LH surge response. An LH surge was defined according to Herbison et al (Herbison et al., 2008) as LH levels greater than two standard deviations above the LH baseline level. WT ovariectomized/sex-steroid replaced mice had baseline LH levels of 1.59 ± 0.95 ng/ml ($n = 6$) at 1500 h reflecting negative feedback that then increased to 13.63 ± 1.17 ng/ml ($n = 7$) at 1600 h (Fig. 6). All WT mice sacrificed at 1600 h had LH levels that met the criteria for an LH surge value (>6.07 ng/ml). In contrast, ovariectomized/sex steroid-replaced *Axl/Tyro3* null mice had more variable baseline LH levels at 1500 h [3.09 ± 1.15 ng/ml (range 0.20 to 6.84, $n = 6$)]. Across the time of the expected LH surge, LH levels at 1600 hr (5.82 ± 1.27 ng/ml, $n=8$) in *Axl/Tyro3* null mice were significantly lower than WT levels (13.63 ± 1.17 ng/ml), suggesting a defect in the sex steroid positive feedback mechanism. Fewer than half of the values met the defined criteria of a significant LH surge when compared to the average baseline LH level (i.e., >8.73 ng/ml) before decreasing again at 1800 hr: 1 of 8 mice (13%) examined at 1600 hr and 4 of 9 mice (44%) at 1700 hr.

Taken together these data suggest that the absence of AXL and TYRO3 is associated with an inability to *consistently* mount a GnRH-induced LH surge in response to increasing sex steroid hormones. These data are complementary to our previous data showing protracted irregular estrous cycles in *Axl/Tyro3* null mice (Pierce et al., 2008) and support the hypothesis that a central defect underlies the reproductive phenotype.

Discussion

TAM family members have been previously shown to play important roles in immune and reproductive functions. Our recent studies demonstrated the importance of AXL and TYRO3 in GnRH neuronal migration, survival and an intriguing reproductive phenotype of delayed first estrous and abnormal estrous cyclicity (Pierce et al., 2008). Whereas vaginal opening is dependent on cumulative tonic GnRH-induced gonadotropin activation of ovarian estrogen production, first estrus is dependent on a normal GnRH-induced LH surge mechanism (Herbison, 2008). We hypothesized that the loss of GnRH neurons in the critical OVLT region of *Axl/Tyro3* null mice disrupted the regular pre-ovulatory LH surge and caused prolonged proestrus. Our previous studies demonstrated a hypothalamic region selective loss of a subset of GnRH neurons during embryogenesis, due to increased apoptotic cell death (Pierce et al., 2008). The current studies further characterize the reproductive phenotype and point toward central abnormalities in GnRH and ability to trigger gonadotropin release rather than potential direct pituitary or gonadal deficits as the site of the mechanism(s) controlling impaired ovarian cyclicity.

Although the TAM family members are expressed in the ovary, the *Axl/Tyro3* null mice had generally normal ovarian histology with similar numbers of corpora lutea and atretic follicles. In addition, the follicle morphology was normal. The trend to a slight increase in number of primary follicles and slight decrease in the number of antral follicles positive for FoxoA in the *Axl/Tyro3* null ovaries was not significant ($P=NS$). The TAM family members were previously shown to be localized to granulosa cells and possibly oocytes in the ovary (Wu et al., 2008), but their precise function is unknown. It is possible that MER, the TAM family member which has been shown to play a major role in apoptotic cell clearance in other systems (Lemke and Rothlin, 2008, Lemke and Lu, 2003), compensates for the absence of AXL and TYRO3 in the gonad, although we found no evidence of up-regulation of MER at the mRNA or protein level. Importantly, mice deficient in *Axl* and *Tyro3* demonstrated a relatively normal ovarian response to graded doses of hCG after PMS in a superovulation protocol suggesting the previously observed estrous cycle abnormalities are unlikely to be caused by a primary gonadal defect. The lack of major ovarian defects was further supported by the relatively normal expression patterns of selected genes that are indicators of

functional granulosa cells and luteal cells in growing follicles and corpora lutea, respectively.

Intact random cycling mice had LH and FSH levels similar to WT, and had a robust response to exogenous GnRH, suggesting no defect in the ability to secrete gonadotropins. However, in the ovariectomy and sex hormone replacement paradigm, *Axl/Tyro3* null mice failed to exhibit a robust sex steroid-induced LH surge. These experiments confirm that the *Axl/Tyro3* null mice have a central defect that is consistent with a decrease in a GnRH-induced LH release that could contribute to their altered estrous cyclicity and persistent proestrous. These effects may be due to the selective loss of a subpopulation of GnRH neurons previously detected in the region surrounding the OVLT (Pierce et al., 2008).

The overall phenotype and reproductive defects in *Axl/Tyro3* mice are different from the GNR23 homozygous mice reported by Herbison and coworkers (Herbison et al., 2008). The GNR23 females were either subfertile or nonfertile, exhibited no corpora lutea, and were unable to generate LH surges. The GNR23 mice, however, had a more dramatic loss of the GnRH neuronal population (Herbison et al., 2008). Similarly, hypogonadal mice (HPG) mice with a deletion in the GnRH gene were reported to have cyclicity restored with only a few GnRH neurons suggesting redundancy in the system (Krieger, Perlow, Gibson et al., 1982, Gibson, 1986). However, these reports also suggested that the rescued HPG mice did not regain normal cyclicity, but became reflex ovulators (Charlton, 2004).

In our studies, the *Axl/Tyro3* null mice have a more limited, but regionally specific loss of GnRH neurons with accompanying increased rates of apoptosis detected by immunoreactive activated caspase-3 (Pierce et al., 2008). Despite these defects, however, these mice are ultimately fertile and have normal litters when housed as breeding pairs. Whether their inability to mount an LH surge is of a variable penetrance or if their ultimate fertility is related to reflex ovulation as in the hypogonadal mouse model is unknown. Initial reports on the *Axl/Tyro3* null animals reported “normal fertility” in females (Lu et al., 1999) and suggested to some that further analysis of their role in reproduction was not warranted. However, in this case as in other mutant mouse models, careful physiologic studies were necessary to detect the more subtle reproductive defects. Collectively, data from various mutant mouse models suggest that it is not solely a specific number of GnRH neurons required for normal reproductive function but importantly, the region-specific location of the neurons that determines the phenotype. As additional factors important in GnRH neuronal migration, survival and later function during development are characterized, our understanding of the complexities of the control of the reproductive axis will expand.

In addition to the importance of the complement of GnRH neurons and their regional specification, other components of the normal GnRH-induced LH surge mechanism remain to be elucidated. Estrogens and possibly progestins are thought to divergently modulate kisspeptin neurons in the anteroventral periventricular preoptic area and the arcuate nuclei (Adachi et al., 2007, Herbison, 2008, Mayer et al., 2010, Gottsch, Clifton and Steiner, 2006, Smith, Clay, Caraty et al., 2007, Roa and Tena-Sempere, 2007, Maeda, Adachi, Inoue et al., 2007, Rothman and Wierman, 2007, Roa, Vigo, Castellano et al., 2006). Since *Axl/Tyro3* mice had variable LH levels in response to castration and steroid replacement, as well as variable ability to mount an LH surge, it raises the possibility of additional sites of action for TAM family members in these regions as a focus for future studies.

Acknowledgments

Thanks to DN Rao Veeramachaneni at Colorado State University for help in the initial review of ovarian morphology, to the members of the Rhodes lab for their comments, to Robert Porteous of the University of Otago School of Medical Sciences, Dunedin, New Zealand for advice regarding the LH surge experimental procedure and

to Dow Corning for gift of Silastic adhesive and tubing. The authors also thank Claire (Yuet) Lo for conducting the *in situ* localization studies and the Microscopy Core at Baylor College of Medicine (Michael Mancini, Director) for use of their imaging facilities.

Grants: HD31191 (MEW) and DC009034 (SAT) These studies were funded in part by NIH-HD-16229 (JSR) and the NIH-HD-04975 (Project 2) that is part of the Baylor College of Medicine SCCPIR (Specialized Cooperative Centers Program in Infertility and Reproduction).

References

- [1]. Lai C, Lemke G. An extended family of protein-tyrosine kinase genes differentially expressed in the vertebrate nervous system. *Neuron*. 1991; 6:691–704. [PubMed: 2025425]
- [2]. Lemke G, Rothlin CV. Immunobiology of the TAM receptors. *Nat Rev Immunol*. 2008; 8:327–36. [PubMed: 18421305]
- [3]. Linger RMA, Keating AK, Earp HS, Graham DK. TAM receptor tyrosine kinases: biologic functions, signaling, and potential therapeutic targeting in human cancer. *Adv Cancer Res*. 2007 in press.
- [4]. Manfioletti G, Brancolini C, Avanzi G, Schneider C. The protein encoded by a growth arrest-specific gene (gas6) is a new member of the vitamin K-dependent proteins related to protein S, a negative coregulator in the blood coagulation cascade. *Mol Cell Biol*. 1993; 13:4976–85. [PubMed: 8336730]
- [5]. Hafizi S, Dahlback B. Gas6 and protein S. Vitamin K-dependent ligands for the Axl receptor tyrosine kinase subfamily. *Febs J*. 2006; 273:5231–44. [PubMed: 17064312]
- [6]. Fang Z, Xiong X, James A, Gordon DF, Wierman ME. Identification of novel factors that regulate GnRH gene expression and neuronal migration. *Endocrinology*. 1998; 139:3654–7. [PubMed: 9681520]
- [7]. Allen MP, Linseman DA, Udo H, Xu M, Schaack JB, Varnum B, Kandel ER, Heidenreich KA, Wierman ME. Novel mechanism for gonadotropin-releasing hormone neuronal migration involving Gas6/Ark signaling to p38 mitogen-activated protein kinase. *Mol Cell Biol*. 2002; 22:599–613. [PubMed: 11756555]
- [8]. Allen MP, Zeng C, Schneider K, Xiong X, Meintzer MK, Bellosta P, Basilico C, Varnum B, Heidenreich KA, Wierman ME. Growth arrest-specific gene 6 (Gas6)/adhesion related kinase (Ark) signaling promotes gonadotropin-releasing hormone neuronal survival via extracellular signal-regulated kinase (ERK) and Akt. *Mol Endocrinol*. 1999; 13:191–201. [PubMed: 9973250]
- [9]. Pierce A, Bliesner B, Xu M, Nielsen-Preiss S, Lemke G, Tobet S, Wierman ME. Axl and Tyro3 modulate female reproduction by influencing gonadotropin-releasing hormone neuron survival and migration. *Mol Endocrinol*. 2008; 22:2481–95. [PubMed: 18787040]
- [10]. Adachi S, Yamada S, Takatsu Y, Matsui H, Kinoshita M, Takase K, Sugiura H, Ohtaki T, Matsumoto H, Uenoyama Y, Tsukamura H, Inoue K, Maeda K. Involvement of anteroventral periventricular metastin/kisspeptin neurons in estrogen positive feedback action on luteinizing hormone release in female rats. *J Reprod Dev*. 2007; 53:367–78. [PubMed: 17213691]
- [11]. Herbison AE. Estrogen positive feedback to gonadotropin-releasing hormone (GnRH) neurons in the rodent: the case for the rostral periventricular area of the third ventricle (RP3V). *Brain Res Rev*. 2008; 57:277–87. [PubMed: 17604108]
- [12]. Mayer C, Acosta-Martinez M, Dubois SL, Wolfe A, Radovick S, Boehm U, Levine JE. Timing and completion of puberty in female mice depend on estrogen receptor alpha-signaling in kisspeptin neurons. *Proc Natl Acad Sci U S A*. 2010; 107:22693–8. [PubMed: 21149719]
- [13]. Lu Q, Gore M, Zhang Q, Camenisch T, Boast S, Casagrande F, Lai C, Skinner MK, Klein R, Matsushima GK, Earp HS, Goff SP, Lemke G. Tyro-3 family receptors are essential regulators of mammalian spermatogenesis. *Nature*. 1999; 398:723–8. [PubMed: 10227296]
- [14]. Schulz NT, Paulhiac CI, Lee L, Zhou R. Isolation and expression analysis of tyro3, a murine growth factor receptor tyrosine kinase preferentially expressed in adult brain. *Brain Res Mol Brain Res*. 1995; 28:273–80. [PubMed: 7723626]
- [15]. Wang H, Chen Y, Ge Y, Ma P, Ma Q, Ma J, Wang H, Xue S, Han D. Immunoeexpression of Tyro 3 family receptors--Tyro 3, Axl, and Mer--and their ligand Gas6 in postnatal developing mouse testis. *J Histochem Cytochem*. 2005; 53:1355–64. [PubMed: 15956026]

- [16]. Wu H, Tang H, Chen Y, Wang H, Han D. High incidence of distal vaginal atresia in mice lacking Tyro3 RTK subfamily. *Mol Reprod Dev.* 2008; 75:1775–82. [PubMed: 18393392]
- [17]. Robker RL, Richards JS. Hormone-induced proliferation and differentiation of granulosa cells: a coordinated balance of the cell cycle regulators cyclin D2 and p27Kip1. *Mol Endocrinol.* 1998; 12:924–40. [PubMed: 9658398]
- [18]. Richards JS, Sharma SC, Falender AE, Lo YH. Expression of FKHR, FKHL1, and AFX genes in the rodent ovary: evidence for regulation by IGF-I, estrogen, and the gonadotropins. *Mol Endocrinol.* 2002; 16:580–99. [PubMed: 11875118]
- [19]. Hsieh M, Mulders SM, Friis RR, Dharmarajan A, Richards JS. Expression and localization of secreted frizzled-related protein-4 in the rodent ovary: evidence for selective up-regulation in luteinized granulosa cells. *Endocrinology.* 2003; 144:4597–606. [PubMed: 12960062]
- [20]. Liu Z, Rudd MD, Hernandez-Gonzalez I, Gonzalez-Robayna I, Fan HY, Zeleznik AJ, Richards JS. FSH and FOXO1 regulate genes in the sterol/steroid and lipid biosynthetic pathways in granulosa cells. *Mol Endocrinol.* 2009; 23:649–61. [PubMed: 19196834]
- [21]. Melaragno MG, Cavet ME, Yan C, Tai LK, Jin ZG, Haendeler J, Berk BC. Gas6 inhibits apoptosis in vascular smooth muscle: role of Axl kinase and Akt. *J Mol Cell Cardiol.* 2004; 37:881–7. [PubMed: 15380678]
- [22]. Prevot V, Lomniczi A, Corfas G, Ojeda SR. erbB-1 and erbB-4 receptors act in concert to facilitate female sexual development and mature reproductive function. *Endocrinology.* 2005; 146:1465–72. [PubMed: 15591145]
- [23]. Heger S, Mastronardi C, Dissen GA, Lomniczi A, Cabrera R, Roth CL, Jung H, Galimi F, Sippell W, Ojeda SR. Enhanced at puberty 1 (EAP1) is a new transcriptional regulator of the female neuroendocrine reproductive axis. *J Clin Invest.* 2007; 117:2145–54. [PubMed: 17627301]
- [24]. Herbison AE, Porteous R, Pape JR, Mora JM, Hurst PR. Gonadotropin-releasing hormone neuron requirements for puberty, ovulation, and fertility. *Endocrinology.* 2008; 149:597–604. [PubMed: 18006629]
- [25]. Lemke G, Lu Q. Macrophage regulation by Tyro 3 family receptors. *Curr Opin Immunol.* 2003; 15:31–6. [PubMed: 12495730]
- [26]. Krieger DT, Perlow MJ, Gibson MJ, Davies TF, Zimmerman EA, Ferin M, Charlton HM. Brain grafts reverse hypogonadism of gonadotropin releasing hormone deficiency. *Nature.* 1982; 298:468–71. [PubMed: 7045700]
- [27]. Gibson MJ. Role of the preoptic area in the neuroendocrine regulation of reproduction: an analysis of functional preoptic homografts. *Ann N Y Acad Sci.* 1986; 474:53–63. [PubMed: 3107453]
- [28]. Charlton H. Neural transplantation in hypogonadal (hpg) mice - physiology and neurobiology. *Reproduction.* 2004; 127:3–12. [PubMed: 15056765]
- [29]. Gottsch ML, Clifton DK, Steiner RA. Kisspeptin-GPR54 signaling in the neuroendocrine reproductive axis. *Mol Cell Endocrinol.* 2006; 254–255:91–6.
- [30]. Smith JT, Clay CM, Caraty A, Clarke IJ. KiSS-1 messenger ribonucleic acid expression in the hypothalamus of the ewe is regulated by sex steroids and season. *Endocrinology.* 2007; 148:1150–7. [PubMed: 17185374]
- [31]. Roa J, Tena-Sempere M. KiSS-1 system and reproduction: comparative aspects and roles in the control of female gonadotropic axis in mammals. *Gen Comp Endocrinol.* 2007; 153:132–40. [PubMed: 17324425]
- [32]. Maeda K, Adachi S, Inoue K, Ohkura S, Tsukamura H. Metastin/kisspeptin and control of estrous cycle in rats. *Rev Endocr Metab Disord.* 2007; 8:21–9. [PubMed: 17377846]
- [33]. Rothman MS, Wierman ME. The role of gonadotropin releasing hormone in normal and pathologic endocrine processes. *Curr Opin Endocrinol Diabetes Obes.* 2007; 14:306–10. [PubMed: 17940457]
- [34]. Roa J, Vigo E, Castellano JM, Navarro VM, Fernandez-Fernandez R, Casanueva FF, Dieguez C, Aguilar E, Pinilla L, Tena-Sempere M. Hypothalamic expression of KiSS-1 system and gonadotropin-releasing effects of kisspeptin in different reproductive states of the female Rat. *Endocrinology.* 2006; 147:2864–78. [PubMed: 16527840]

- [35]. Bellosta P, Costa M, Lin DA, Basilico C. The receptor tyrosine kinase ARK mediates cell aggregation by homophilic binding. *Mol Cell Biol.* 1995; 15:614–25. [PubMed: 7823930]
- [36]. Costa M, Bellosta P, Basilico C. Cleavage and release of a soluble form of the receptor tyrosine kinase ARK in vitro and in vivo. *J Cell Physiol.* 1996; 168:737–44. [PubMed: 8816929]

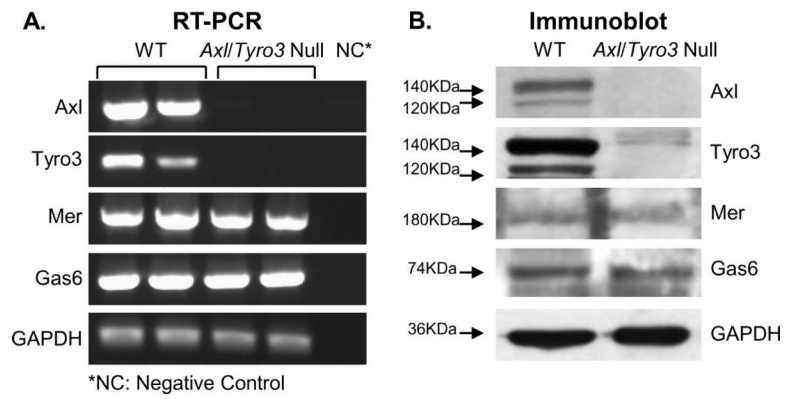


Fig 1. Expression of TAM family members and their ligand in WT and *Axl/Tyro3* null ovaries. Panel A: mRNA levels were measured by semi quantitative RT-PCR amplification of *Axl*, *Tyro3*, *Mer*, and *Gas6* transcripts isolated from total ovarian RNA. Panel B: Protein levels displayed by immunoblot of ovarian lysates. Both AXL and TYRO3 exhibit doublet bands at approximately 120 and 140 KDa (Bellosta, Costa, Lin et al., 1995, Costa, Bellosta and Basilico, 1996) (note faint larger bands from nonspecific binding of Tyro3 antibody) (Lai and Lemke, 1991). GAPDH was used as an internal control.

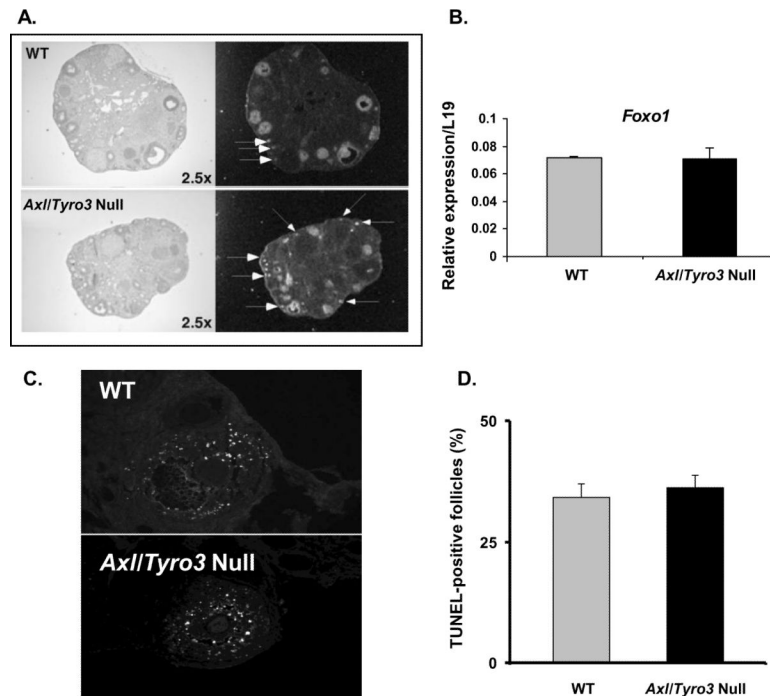


Fig. 2. Follicular development in WT and *Axl/Tyro3* null ovaries. Panel A: Images of *in situ* hybridization shows *Foxo1* mRNA in oocytes and granulosa cells of growing follicles present in ovaries of both groups. *Foxo1* signals present in oocytes are denoted by the white arrows; other signals are exclusively in granulosa cells. Panel B: The graph shows a comparison of *Foxo1* mRNA levels in WT (n = 4) and *Axl/Tyro3* null (n = 6) ovaries. Panel C: Apoptosis in pre-antral and antral follicles. TUNEL-positive follicles from both groups were histologically similar. Sections were examined and digital images were acquired using a 20 \times objective. Panel D: The percentage of growing follicles that were TUNEL positive is shown for WT (n = 4) and *Axl/Tyro3* null (n = 4) mice.

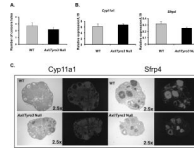


Fig. 3.

Markers of luteal function. Panel A: The graph depicts the number of corpora lutea observed in representative cross sections obtained from WT and *Axl/Tyro3* null ovaries. Panel B: Comparison of *Cyp11a1* and *Sfrp4* mRNA levels in WT (n = 4) and *Axl/Tyro3* null (n = 6) ovaries. Panel C: Images from *in situ* localization show *Cyp11a1* and *Sfrp4* mRNAs in corpora lutea present in ovaries of both groups. *Cyp11a1* expression is shown in the left-hand panels; those for *Sfrp4* are on the right. Expressed mRNAs are clearly visible as the dark silver grains in the bright field images and by the white areas in the dark field images.

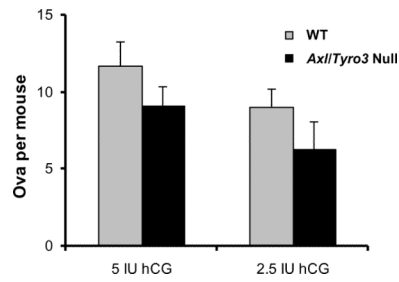


Fig. 4. Ovarian response to exogenous gonadotropins. The graph depicts the number of ova collected after standard protocol of HMG followed by either 5 IU hCG (WT n = 7, *Axl/Tyro3* null, n = 8) or 2.5 IU hCG (WT n = 8, *Axl/Tyro3* null, n = 10) (see methods for details).

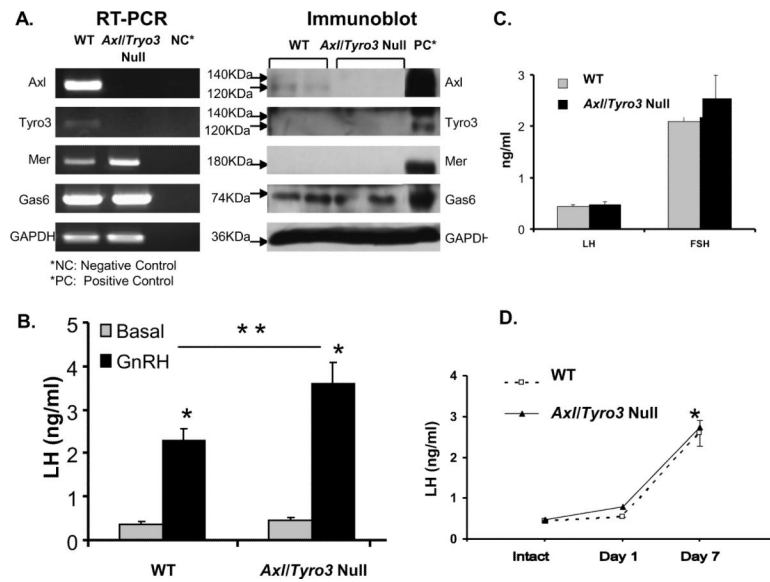


Fig. 5. Pituitary TAM expression and function. Panel A: Expression of TAM family members and their ligand in WT and *Axl/Tyro3* null pituitaries. Panel B: LH levels following GnRH administration (200 ng/kg s.c.) in intact WT (n = 8) and *Axl/Tyro3* null (n = 9) female mice. Hormone levels were determined on trunk blood as described in Methods. Panel C: LH and FSH levels in intact WT and *Axl/Tyro3* null mice. For LH levels, vaginal smears were performed on random cycling WT (n = 12) and *Axl/Tyro3* null (n = 18) mice and mice sacrificed during diestrous and proestrous. For FSH levels, WT (n = 5) and *Axl/Tyro3* null (n = 6) random cycling mice were sacrificed in the morning. Panel D: LH levels post ovariectomy in WT and *Axl/Tyro3* null female mice (n = 4 and 6, respectively at day 7, *p < 0.05, **p < 0.01, see methods for details).

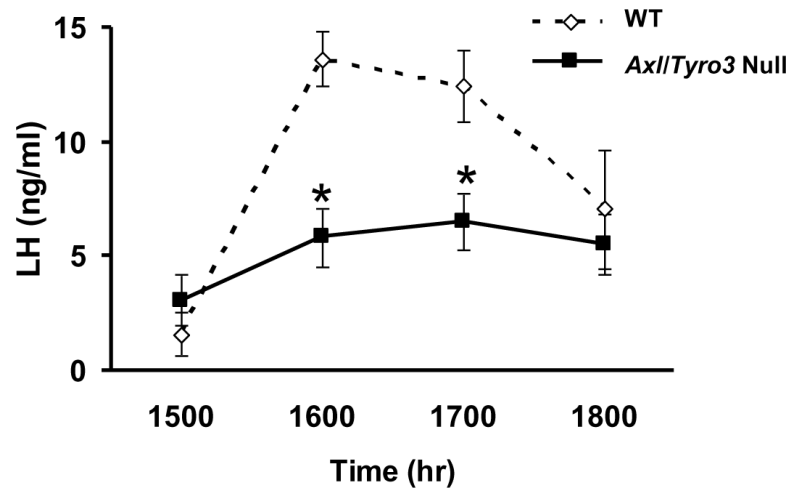


Fig. 6. *Axl/Tyro3* null mice are unable to mount a normal LH surge. The graph depicts LH levels in groups of mice after ovariectomy and sex hormone replacement. At the 1500, 1600, 1700, and 1800 time-points, WT n = 6, 7, 7 and 6 and *Axl/Tyro3* null n = 6, 8, 9 and 8, respectively. Mean LH levels \pm SEM in WT (dashed line) and *Axl/Tyro3* null (solid line) mice (* p <0.05, see methods for details).